

N O T I C E

THIS DOCUMENT HAS BEEN REPRODUCED FROM
MICROFICHE. ALTHOUGH IT IS RECOGNIZED THAT
CERTAIN PORTIONS ARE ILLEGIBLE, IT IS BEING RELEASED
IN THE INTEREST OF MAKING AVAILABLE AS MUCH
INFORMATION AS POSSIBLE



Technical Memorandum 80588

Implications of Cyclotron Features in the X-Ray Spectrum of HER: X-1

R. Bussard

(NASA-TM-80588) IMPLICATIONS OF CYCLOTRON
FEATURES IN THE X-RAY SPECTRUM OF HER X-1
(NASA) 48 p HC A03/MF A01 CSCL 03B

N80-12989

G3/93 Unclassified
41487

MAY 1979

National Aeronautics and
Space Administration

Goddard Space Flight Center
Greenbelt, Maryland 20771



Implications of Cyclotron Features In The X-Ray Spectrum Of Her X-1

R. W. Bussard*
Laboratory for High Energy Astrophysics
NASA/Goddard Space Flight Center
Greenbelt, MD 20771

Abstract:

We have investigated the modification of physical processes due to an intense magnetic field to uncover implications for X-ray spectra from binary pulsars. We find that for large enough fields, the quantum nature of electron orbits must be taken into account, and for densities typical of binary X-ray pulsars, we find that electrons spend most of their time in the ground state. For this case, we have estimated the production of cyclotron line photons following collisional excitation and considered the effects of the transfer of line photons through the hot plasma. A line feature as narrow as reported (Trümper et al., 1977 and 1978) appears unlikely. However, more recent observations allow a much broader line, and in addition, a consistent absorption feature due to knock-on electrons may explain the spectral steepening at ~ 20 keV.

*Also Department of Physics and Astronomy, University of Maryland

I. Introduction

Pulsars with periods in the range from tens of milliseconds to seconds are believed to be spinning neutrino stars with strong magnetic fields rigidly anchored to their surfaces. The pulse period corresponds to the rotation period, and in the case of isolated radio pulsars, the rate of change of the period is consistent with the radiative energy lost by a spinning magnetic dipole. In this context, typically, the strength of the magnetic field is estimated to be $\sim 10^{12}$ G. Fields of this strength alter considerably the interactions of electrons with both radiation and ions, primarily by restricting the allowed electron recoil transverse to the field. Radiative transitions between quantum levels give rise to cyclotron line emission and absorption, and the Coulomb scattering process becomes highly modified because of the restricted momentum transfer to the electron. The line processes have been treated in detail by Daugherty and Ventura (1977 and 1978); the Compton scattering cross section for low energy photons ($\omega \ll eB/(m_e c)$) was calculated by Canuto, Lodenquai and Ruderman (1971). Resonances in the non-relativistic Coulomb electron-ion collision frequency were discovered by Ventura (1973). Current X-ray observations, however, require more refined calculations of the collisional cross sections. In this paper, we have calculated an effective scattering cross section for line photons and the Coulomb cross section for electron-ion collisions, treating the electrons relativistically.

In section II, we discuss the quantization of electron orbits in strong fields, and show that under the conditions expected at the polar

caps of X-ray pulsars, electrons will likely spend most of their time in the magnetic ground state, corresponding to zero pitch angle. Then, using a fully relativistic quantum electrodynamic approach, we calculate the electron-ion Coulomb cross section and the absorption cross sections and emission rates for cyclotron photons. Recent evidence has been presented for a cyclotron emission line feature at about 60 keV in the spectrum of Hercules X-1, an X-ray pulsar in a binary system (Trümper et al., 1977 and 1978, Coe et al., 1977). In order to explore implications of this data, in section III, we have applied the cross sections developed above to the situation where matter accretes onto the magnetic polar cap of a neutron star. We calculate an upper limit to the multiplicity of cyclotron line photons produced by an accreting proton, and we present a rate coefficient for line production in a thermal plasma. Section IV consists of an application of our results to the data from Hercules X-1. In particular, we consider the production rates of the cyclotron emission line mentioned above and its transfer through a hot plasma. The line width is estimated as a function of the angle between our line of sight and the magnetic field lines, and we find the reported best fit line width (Trümper et al., 1978) places stringent requirements on the viewing angle. We also present an interpretation of the spectral steepening at ~ 20 keV in terms of an absorption feature which is consistent with line observations. Finally, in section V, we summarize our results and indicate the need for further observations.

II. The Effects of Quantization in Intense Magnetic Fields

The Dirac equation for the spinors ψ representing electrons in an external static and homogeneous magnetic field is, in units where $\hbar = c = 1$,

$$(\gamma^\mu \pi_\mu - m_e) \psi(x) = 0, \quad \mu = 0 \text{ to } 3, \quad (1)$$

where m_e is the electron mass, γ^μ are the Dirac matrices, and

$$\pi_\mu = i \frac{\partial}{\partial x^\mu} + e A_\mu(x); \quad (2)$$

$$A_0 = 0 \text{ and } \vec{A} = \frac{1}{2} \vec{B} \times \vec{x} \quad (3)$$

The eigenvalues of total energy W are given by

$$W^2 = p^2 c^2 + m_e^2 c^4 \left(1 + \frac{2B}{B_q} j\right), \quad j = 0, 1, 2, \dots \quad (4)$$

where p is the electron momentum parallel to the field, c is the speed of light, m_e is the mass of the electron, and in cgs units,

$$B_q = \frac{m_e^2 c^3}{e \hbar} = 4.413 \times 10^{13} \text{ Gauss.} \quad (5)$$

The corresponding spinors for a particular positive energy state, assuming B lies in the z -direction, are

$$\psi(x) = 2LW(W + m_e)^{-\frac{1}{2}} (\gamma^\mu \pi_\mu + m_e) f_{j-s-\frac{1}{2}, q}(\vec{x}_\perp) e^{-iWt + ipz} u_s; \quad q=0, 1, 2, \dots \quad (6)$$

where L is the normalization length, \vec{x}_\perp is the projection of the position vector into a plane perpendicular to the field, s is the spin of the electron, and

$$U_{\frac{1}{2}} = \begin{matrix} 1 \\ 0 \\ 0 \\ 0 \end{matrix} \quad U_{-\frac{1}{2}} = \begin{matrix} 0 \\ 1 \\ 0 \\ 0 \end{matrix} \quad (7)$$

The quantum number j labels the angular momentum parallel to the field from the contributions of spin and orbit around the guiding center, while q gives the distance from the guiding center to the z -axis of the chosen coordinate system. The functions $f_{nq}(\vec{x}_\perp)$ are defined most conveniently by the ladder operators:

$$\begin{aligned}\pi^\pm &= \frac{1}{\sqrt{2}} (\pi^x \pm i \pi^y) \text{ and} \\ x_\perp^\pm &= \frac{1}{\sqrt{2}} (x_\perp \pm i y_\perp) \pm \frac{i}{eB} \pi^\pm;\end{aligned}\quad (8)$$

then

$$\pi^\pm f_{nq}(\vec{x}_\perp) = [eB(n + \frac{1}{2} \pm \frac{1}{2})]^{1/2} f_{n \pm 1, q}(\vec{x}_\perp) \quad (9)$$

and

$$x_\perp^\pm f_{nq}(\vec{x}_\perp) = [\frac{q + \frac{1}{2} \mp \frac{1}{2}}{eB}]^{1/2} f_{n, q \mp 1}(\vec{x}_\perp), \quad (10)$$

together with

$$f_{00}(\vec{x}_\perp) = \left(\frac{eB}{2\pi}\right)^{1/2} \exp\left(-\frac{eB}{4} \vec{x}_\perp^2\right) \quad (11)$$

define the functions completely. The π operators correspond to the canonical momentum of the electron and the X operators to the coordinates of the guiding center. There are two contributions to the transverse energy quantum number j , expressed by setting

$$j = n + s + \frac{1}{2}, \quad n = 0, 1, 2, \dots, \quad s = \pm \frac{1}{2} \quad (12)$$

Then n refers to the Landau level, the state of the orbital motion of the electron about its guiding center, and s is the contribution of spin to the magnetic moment. Note that only $s = -1/2$ is permitted for the ground state.

In a magnetic field, radiation can be emitted and absorbed accompanying transitions between transverse energy levels. Under normal astrophysical conditions, particle energies are much larger than the energy level separation, and the particles consequently have large parallel momenta and high quantum numbers. This leads to a classical approximation, and while the radiation is still quantized, the large parallel momenta Doppler shift the emitted photons into a continuous synchrotron spectrum. However, even for mildly relativistic electrons ($\gamma \leq 1.1$) in fields greater than 10^{12} gauss, the quantum nature of the emission and absorption of radiation must be taken into account. Discrete cyclotron line emission rates and absorption cross sections have been calculated for intense fields by Daugherty and Ventura (1977 and 1978). We have repeated these calculations in the representation above, which is somewhat different from theirs. The QED matrix element for a transition is given by

$$S_{fi} = ie \int d^4x \bar{\psi}_f(x) \vec{\nabla} \cdot \vec{A}_1(x) \psi_i(x) \quad (13)$$

where the subscripts f and i refer to final and initial states and $\vec{A}_1(x)$ is the photon vector potential, given by

$$\vec{A}_1(x) = \frac{2\pi}{\omega V} \frac{1}{2} \hat{\epsilon} e^{\pm i(\omega t - \vec{k} \cdot \vec{x})}, \quad \begin{array}{l} - \text{ for absorption} \\ + \text{ for emission} \end{array} \quad (14)$$

where ω and \vec{k} are the photon frequency and wave-vector, $\hat{\epsilon}$ is the polarization vector, and V is the normalization volume. The bar over ψ_f indicates the Pauli adjoint of the spinor, $\psi_f^\dagger \gamma^0$.

We have confirmed the results of Daugherty and Ventura (1977 and 1978) for the absorption cross sections and emission rates using the

ladder operator representation in cylindrical coordinates. For example, the cross section for an electron in the ground state to absorb a fundamental cyclotron photon is given here in the center of parallel momentum frame, where the sum of the parallel momenta of the photon and electron vanishes:

$$\begin{aligned}\sigma_a(\omega, \theta) = & \frac{\pi^3 e^2}{\omega} \frac{\delta(W_i + \omega - W_1) e^{-\xi}}{W_1 (W_1 + m_e) (W_i + m_e)} (m_e^2 + 2W_1 \omega \cos^2 \theta)^{-\frac{1}{2}} \\ & \{ \delta_{s_f, \frac{1}{2}} 2m_e^2 \frac{B}{B_q} ((W_1 + m_e) \xi + W_i + m_e)^2 \cos^2 \theta \epsilon_o^2 + (W_1 + m_e)^2 \epsilon_x^2 \} \\ & + \delta_{s_f, \frac{1}{2}} \omega^3 [(W_i + m_e + \omega \cos^2 \theta)^2 \epsilon_o^2 + (W_1 + m_e)^2 \cos^2 \theta \epsilon_x^2] \} \quad (15)\end{aligned}$$

where θ is the angle of propagation of the photon and ω its frequency, and

$$W_1 = m_e \left(1 + \frac{2B}{B_q}\right)^{\frac{1}{2}} \quad (16)$$

$$W_i = (m_e^2 + \omega^2 \cos^2 \theta)^{\frac{1}{2}} \quad (17)$$

$$\xi = \frac{B_q}{2B} \frac{\omega^2}{m_e^2} \sin^2 \theta \quad (18)$$

ϵ_o and ϵ_x are the polarization amplitudes in the ordinary (wave's electric field parallel to B) and extraordinary modes, respectively.

As we shall now discuss, this cross section is of particular importance for intense magnetic fields, since it will determine the opacity in the line feature. We note that equation (15) differs from the classical result by terms of order B/B_q , which implies that these corrections are important wherever the optical depth exceeds B_q/B .

In a strong field, mildly relativistic electrons will spend most of their time in the ground state, unless the densities are very high. To see this, Figure 1 shows the lifetime τ_1 of the first excited state as a function of field strength for electrons with no parallel velocity. This was calculated by numerically integrating over all photon transitions to the ground state, according to

$$\tau_1 = \left(\sum_c \int d^3k R_{01}(\vec{k}, \epsilon) \right)^{-1} \quad (19)$$

where $R_{01}(\vec{k})d^3k$ is the rate per electron of photon emission into d^3k centered about \vec{k} and is calculated in the appendix. As mentioned before, there are two possible spin orientations for the excited states; the lifetime of each is shown separately in the figure. For low enough densities, collisional excitation times will be much longer than radiative lifetimes; we will return to this after calculating the collisional cross sections.

In a Coulomb collision, the momentum transfer prefers to occur perpendicular to the relative velocity. For energetic protons with small pitch angle colliding with an electron in the ground state of an intense field, the transfer of energy to the electronic plasma is inhibited (Basko and Sunyaev 1975). However, under energetically favorable conditions, the proton can transfer transverse momentum to the electron by excitation of the quantum levels. In addition, head-on or knock-on collisions can occur, in which the electrons are not excited, but are reflected along their field line. We have calculated the cross sections for these processes as a function of the electron energy in the proton's rest frame by a single photon exchange approximation. The matrix element is given by

$$S_{fi} = -ie \int d^4x \overline{\psi_f(x)} \gamma^0 A_0^{(c)}(x) \psi_i(x) \quad (20)$$

where $A_0^{(c)}(x)$ is the Coulomb potential due to the ion charge. After a Fourier decomposition of this potential as outlined in the appendix, we find the cross section σ_j for excitation of the j th state from the ground state in a Coulomb collision with an ion of charge Ze with zero pitch angle is given in the ion's rest frame by (in cgs units)

$$\sigma_j(p) = \frac{\pi B q}{2B} \frac{Z^2 r_e^2}{(W+m_e c^2)^2} \frac{1}{j!} \sum_{\pm} |p c p'_{\pm} c|^{-1} \{ \delta_{s'}, -\frac{1}{2} [2W(W+m_e c^2) + p c (p'_{\pm} - p) c]^2 + \delta_{s', \frac{1}{2}} \frac{2B}{B q} j m_e^2 c^4 p^2 c^2 \} \epsilon_j \left(\frac{B q}{2B} \frac{(p'_{\pm} - p)^2}{m_e^2 c^2} \right) \quad (21)$$

where r_e is the classical electron radius, 2.82×10^{-13} cm, p and p' are respectively the initial and final electron momenta parallel to the field, E is the electron kinetic energy, and s' is its final spin. There are two possible values of the final momentum, given by $p'_{\pm} = \pm \sqrt{p^2 - 2m_e^2 c^2 B/B_q} j$, and these are summed over in equation (21).

Finally the ϵ_j are defined by

$$\epsilon_j(x) = \int_x^{\infty} \frac{dt}{t^2} e^{-(t-x)} (t-x)^j \quad (22)$$

The first three are given here in terms of the exponential integral:

$$\begin{aligned} \epsilon_0(x) &= \frac{1}{x} - e^x E_1(x) \\ \epsilon_1(x) &= -1 + (1+x)e^x E_1(x) \\ \epsilon_2(x) &= 1+x - (2+x)x e^x E_1(x). \end{aligned} \quad (23)$$

The $j=0$ cross section refers to knock-on collision where the parallel momentum of the electron changes sign (in the ion's rest frame), but no transverse excitation occurs. Higher j values refer to collisions in which the electron is excited to the j level. These results are shown in Figure 2 for 2 magnetic field strengths, 10^{12} G and 6×10^{12} G. Because of a breakdown in the approximation, the cross sections become infinite at the thresholds of excitation. However, the bandwidth of the breakdown is small, so we have arbitrarily smoothed these infinities. The approximation breaks down because p , the final momentum, becomes small, and the particles are near each other for a long enough time

to exchange more than one virtual photon. These infinities are the resonances discovered by Ventura (1973). As in the non-magnetized case, bound states are even possible. The cross section for deexcitation from level j to the ground state is given by equation (22) with p and p' interchanged on the right hand side.

From Figure 2, we see that above the threshold, the excitation to the $j = 1$ level dominates, so we can find the critical density below which the radiative lifetime of the first excited state is shorter than its collisional deexcitation rate. That is, for densities lower than this critical value electrons will spend most of their time in the ground state. The critical density is defined by

$$n_{cr} = \frac{1}{\sigma_1 v \tau_1} , \quad (24)$$

where σ_1 is given by equation (21), τ_1 by equation (19), and v is the electron velocity. For example, comparing Figures 1 and 2 gives values of $\sim 10^{27} \text{ cm}^{-3}$ ($E > 15 \text{ keV}$) in a field of 10^{12} Gauss , and $\sim 10^{29} \text{ cm}^{-3}$ ($E > 70 \text{ keV}$) in a field of $6 \times 10^{12} \text{ Gauss}$. The X-ray emitting regions even in accreting binary X-ray pulsars are expected to be much less dense than these values. We note also that because the collisional deexcitation cross section is nearly equal to that for excitation, collisional excitation nearly always results in radiative deexcitation.

Under conditions where the electrons occupy the ground state, the opacity in the cyclotron line is determined from the cross section given in equation (15). Since this cross section is much larger than

that for Compton scattering, the possibility arises of a source region optically thick to line photons but not to the surrounding continuum. Since Compton scattering is the most important factor in radiative transfer outside the line process, a line feature will appear in this case. The width of the line can be roughly determined by finding the photon frequency and angle ranges where the optical depth exceeds unity. The optical depth is given by

$$\tau_B(\omega, \theta) = \int dl n_e \int dp f_e(p) \sigma_a(\omega^*, \theta^*) \quad (25)$$

where dl is the line of sight increment, $f_e(p)$ is the electron parallel momentum distribution function, and σ_a is given by equation (15). The asterisk denotes the center of parallel momentum frame. If we assume that the electron spectrum is uniform throughout the source, the δ -function in equation (15) allows us to evaluate the momentum integral to obtain

$$\tau_B(\omega, \theta) = N_e \sum_{\pm} f_e(p_{\pm}) S(\omega^*, \theta^*) \frac{W_1}{\omega} \frac{W_{\pm}}{|W_{\pm} \cos \theta - p_{\pm}|} \quad (26)$$

where N_e is the column density of electrons in the source, p_{\pm} and W_{\pm} are the momenta and total energy which satisfy the line resonance condition, given below, and $S(\omega^*, \theta^*)$ is the right hand side of equation (15) without the δ -function. W_{\pm} and p_{\pm} are solved for from

$$W_{\pm} - p_{\pm} \cos \theta = \frac{1}{2\omega} \left(\frac{2B}{B_q} m_e^2 - \omega^2 \sin^2 \theta \right) \quad (27)$$

which yields:

$$p_{\pm} = \frac{\omega}{2\xi} \left[(1-\xi) \cos \theta \pm \left((1-\xi)^2 - \frac{2B}{B_q} \xi \right)^{1/2} \right], \quad (28)$$

where ξ is defined by equation (18). We note an important

feature: there exists an angular dependent upper bound $\omega_{\max}(\theta)$ on the line energy where the quantity under the square root in equation (28) becomes negative. This limit is given by

$$\omega_{\max} \sin\theta = m_e \left[\left(1 + \frac{2B}{B_q} \right)^{\frac{1}{2}} - 1 \right] \quad (29)$$

To undertake a study of the radiative transfer of the line photons, we note that for $n \ll n_{ex}$, an electron which is excited by absorbing a line photon will deexcite radiatively before anything can happen to change its momentum. Thus, the process is effectively a scattering of the line photon, and so, in a transfer problem, the photon number is conserved. The scattering cross section is the product of the absorption cross section and the probability of emission into a given final angle.

This gives the expression that should be used at the infinite resonance in the Compton scattering cross section of Canuto, Lodenquai, and Ruderman (1971).

III. Cyclotron Line Production in Binary X-ray Pulsars

The X-ray luminosity of pulsars in binary systems with main sequence companions presumably results from accretion. Here we consider the case in which the pulsar magnetic field forces plasma to accrete to a polar cap with nearly zero pitch angle. The X-rays are generated by the interaction of the accretion column falling at its free-fall velocity ($\sim 0.5c$) with the background atmospheric plasma. In a steady state situation, the atmosphere must be hot enough to avoid the two stream instability, or have thermal velocities comparable to the infall velocity, implying temperatures corresponding to tens of keV. In other words, when the atmospheric density is comparable to that in the accretion column, the two stream instability would heat the atmosphere to these temperatures much faster than it could cool.

Under these conditions, if plasma instabilities are not operative, one expects the infalling ions to lose energy in Coulomb processes. However, since momentum transfer prefers to occur perpendicular to the relative velocity vector in a Coulomb encounter, we see that energy losses for zero pitch angle protons will be reduced (Basko and Sunyaev 1975) because transverse momentum cannot be continuously transferred to the background, but must be given up in quanta with $(\Delta p_{\perp})^2 \sim 2m_e^2 c^2 B/B_q$.

To investigate this effect quantitatively, we have used the results of the previous section for the Coulomb cross sections σ_j in an intense magnetic field to calculate the energy loss rate per unit matter traversed for a proton with zero pitch angle by Coulomb processes:

$$\frac{dE}{dx} = \frac{1}{m_p v} \sum_{j=0}^{\infty} \int_{-\infty}^{\infty} dp f_e(p) v_{\text{rel}}(E, p) \sigma_j(E, p) \Delta E_j(E, p) \quad (30)$$

where m_p is the proton mass, v is the proton velocity, p is the electron parallel momentum, f_e is the electron distribution function in p , v_{rel} is the relative velocity between the particles in an encounter, and ΔE_j is the energy lost in the collision. We assume a relativistic one dimensional thermal distribution of electrons, so that $f_e(p)$ is given by

$$f_e(p) = \exp[-(p^2 + m_e^2)^{1/2}/T] / [2m_e K_1(\frac{m_e}{T})] \quad (31)$$

where $K_1(x)$ is the modified Bessel function (Abramowitz and Stegun 1965) and T is the temperature in units of energy. The results are shown in Figure 3 for four temperatures and a field strength of 6×10^{12} G. For comparison the energy loss rate in a non-magnetized gas of temperature 35 keV is shown by the dashed line (Book and Ali 1975) and in a field of 10^{12} G with temperature 15 keV by the dash-dotted line. For $T = 0$, there is a sharp discontinuity at the threshold for excitation, but this disappears when the electrons take on a thermal distribution, and for the higher field strength at $T = 35$ keV, dE/dx is relatively constant in energy. The energy losses may be approximated with the classical formula by replacing the plasma frequency with the cyclotron frequency in the Coulomb logarithm. For a neutral magnetized gas, Lee (1979) has shown that classically the cyclotron frequency should replace the excitation frequency in this term.

Figure 4 shows the Coulomb mean ranges for the temperatures discussed above and a field strength of 6×10^{12} G. As Basko and Sunyaev (1975) pointed out, for high enough energies elastic proton-proton nuclear scattering has a mean free path smaller than the Coulomb range ($x_{p-p, \text{elas}} \sim 50 \text{ gm/cm}^2$). In an elastic scattering, the proton is deflected from zero pitch angle, and then its transverse energy can be given up rapidly to ambient electrons, via the excitation of plasma waves parallel to the field, for example. Thus, the equation for the energetic zero pitch angle proton distribution function is a steady state atmosphere can be written

$$\frac{\partial \Phi}{\partial x} - \frac{\partial}{\partial E} (\Phi \frac{dE}{dx}) = - \frac{\sigma_{pp}(E)}{m_p} \Phi(E, x) \quad (32)$$

where E is the proton energy, x the amount of matter traversed (in gm/cm^2 for example), Φ is the differential (in energy) flux of protons, and σ_{pp} is the cross section for a nuclear collision with an ambient proton, taken from the compilation of Barashenkov and Maltsev (1961). The solution to this equation with the boundary condition that injection occurs at the top of the atmosphere, ($x = 0$) with flux $\Phi_0 \delta(E - E_0)$ is

$$\Phi(E, x) = \Phi_0 / \frac{dE}{dx} \cdot \exp \left[- \int_{E_0}^E \frac{dE' \sigma_{pp}(E')}{m_p dE' / dx} \right] \delta(x - \int_{E_0}^E \frac{dE'}{dE' / dx}) \quad (33)$$

To evaluate the line productivity of the protons in a one dimensional thermal gas, we have integrated the flux given by equation (33) with the cross sections for knock-on and excitation collisions. The production rates at a depth x of electrons in quantum level j with momentum p in dp is given by

$$q_j(p, x) = n_e \int dp' f_e(p') \int_{E_0}^E dE \Phi(E, x) \frac{v_{\text{rel}}(p', E)}{v(E)} \sigma_j(p'^*) \delta(p - p_+(p', E)) \quad (34)$$

where n_e is the electron number density, $\Phi(E, x)$ is the proton flux given by equation (33), $v_{\text{rel}}(E, p')$ is the relative velocity between the particles, $v(E)$ is the velocity of the ion, p'^* is the incident momentum in the ion rest frame, and the momentum in the delta function is obtained from the conservation equations:

$$W^* = W'^*, \quad p_{\pm}^* = \pm \sqrt{p'^*{}^2 - 2eBj}, \quad (35)$$

where the *'s refer to the ion's rest frame. The total column density production rate is found by integrating along dz , the path of the infalling ions:

$$\dot{N}_{e,j}(p) = \int dz q_j(p, x) = \frac{1}{\rho} \int_0^{\infty} dx q_j(p, x) \quad (36)$$

The resulting expression for this quantity, after taking the delta functions into account, is

$$\dot{N}_{e,j}(p) = \frac{n_e}{\rho} q_0 \int_0^{E_0} \sum_{\pm} f_e(p'_{\pm}) \left| \frac{\partial p}{\partial p'} \right|_{p'_{\pm}}^{-1} \sigma_j(p'_{\pm}^*) \frac{v_{\text{rel}}(p'_{\pm}, E)}{v(E)} \exp \left[- \int_E^{E_0} \frac{dE' \sigma_{pp}(E')}{m_p \frac{dE}{dx}} \right] \quad (37)$$

The excitation of an electron to the j th level was assumed to yield j line photons since the electrons tend to deexcite in single step transitions (Canuto and Ventura 1977, Daugherty and Ventura 1977). A knock-on ($j = 0$) was assumed to produce as many line photons as was energetically possible, by Coulomb collisions with ambient ions. It is important to note that here we neglect energy losses of the knock-ons to continuum photons by resonant absorption (Pravdo et al., 1978)

which results in the conversion of these photons to line photons; this process is discussed below. The results for the multiplicity of line photons produced under these assumptions are shown for the four temperatures with $B = 6 \times 10^{12}$ G in Figure 5a, and Figure 5b shows the fraction of the proton's energy put into line photons as a function of the injection energy. For Figure 5b, we assume a line photon has an average energy equal to the energy of the 1st excited state with $p = 0$.

In order to investigate the production of cyclotron line photons by the high energy tail of a one dimensional thermal electron distribution in collisions with ambient protons, we have integrated the cross section for the excitation of the first excited state with such a distribution function. The resulting line production rate per unit gas density squared, α_1 , is given by

$$\alpha_1(T) = \int dp f_e(p) \sigma_1(p) v(p) \quad (38)$$

The results for temperatures of 1 to 100 keV are shown in Figure 6, for field values of 10^{12} and 6×10^{12} Gauss. As can be seen, the line production coefficient α_1 rises quite rapidly as kT approaches $\hbar e B / (m_e c)$ and flattens somewhat at higher temperatures.

As noted above, these results apply to line production by electron-ion collisions alone. However, a photon with energy below the cyclotron energy can collide with a fast ($\beta \sim 0.6$ to 0.8) knock-on electron and be absorbed as a cyclotron photon because of the Doppler shift. When the electron deexcites, the photon tends to be emitted preferentially into the electron's forward hemisphere, or downward

toward the star's surface. The importance of this effect may be twofold: reemission at angles around 90° , since these have little Doppler shift, leads to an increase in line photons; and the absorption results in a depletion of the continuum below the line energy, which could make a line appear more intense relative to continuum radiation. It is difficult to be quantitative about this effect because although the production rate of knock-ons can now be calculated, their momentum spectrum depends also on the energy loss rate to the radiation, the spectrum of which is unknown. It is, however, interesting to note that if the field strength is as high as implied by the data of Trümper et al. (1977 and 1978), $\sim 6 \times 10^{12}$ Gauss, then the knock-on process is the dominant one for producing line photons under the previous assumptions (neglect of radiation). So if now we assume that the knock-ons lose all their energy by converting ~ 30 keV photons to ~ 60 keV photons instead of losing 60 keV per photon produced, the the multiplicity is only increased by at most a factor of 2. The knock-on production rates are strongly dependent on the field strength because of the threshold effect; at lower field values, relatively more direct excitations than knock-ons occur.

IV. Application to Hercules X-1

The results of the calculations in the preceding section of the fractional energy lost by infalling protons to line photons may be compared with recent possible observations of a line feature in the spectrum of Hercules X-1 at around 60 keV (Trümper et al., 1977 and 1978, Coe et al., 1977). Assuming that the line is directly produced

by the infalling ions and the rest of the ion's energy goes into continuum radiation, the calculations leading to Figure 5 will apply if radiative transfer in the source or outside does not convert continuum photons into line photons or vice versa. There are two observed components of continuum radiation, hard (2 to 20 keV) and soft (.1 to 1 keV) X-rays, with roughly comparable luminosities of 1 to 2×10^{37} ergs s^{-1} (Giacconi et al., 1973, Schulman et al., 1975, Catura and Acton 1975), while the observed line luminosity is $\sim 2 \times 10^{35}$ ergs s^{-1} . The infalling protons are generally assumed to power both continuum components, so at most, only 1/2 to 1 percent of the energy comes out in the line. Since the effective hard X-ray temperature is ≥ 20 keV (Pravdo et al., 1977), we see from Figure 5b that this fraction is consistent with infall proton energies of 140 MeV to 180 MeV. However, we still must investigate the effect of radiative transfer, in the source and outside.

To ascertain whether radiative transfer is important, we need to estimate the electron density in the source. From Figure 4, we see that the range of accreting matter is at least of order 10 gm cm^{-2} , corresponding to $\sim 6 \times 10^{24} \text{ e}^{-} \text{ cm}^{-2}$. The reported width of the line feature is 12 keV (FWHM), and this places an upper limit on the linear dimension of the source parallel to the field, since the line energy varies as field strength. The upper limit is obtained from assuming $B \propto R^{-3}$ as for a dipole field:

$$L = \frac{1}{3} R \frac{\Delta B}{B} \approx \frac{1}{3} R \frac{\Delta \omega}{\omega} = 7 \times 10^4 \text{ cm} \left(\frac{R}{10 \text{ km}} \right) \quad (39)$$

where R is the neutron star radius. Thus the lower limit on the average electron density in the source is given by

$$n_e \geq \frac{N_e}{L} \geq 10^{20} \text{ cm}^{-3} \left(\frac{R}{10 \text{ km}} \right)^{-1} \quad (40)$$

From equations (25) and (15), then, we estimate the opacity to be

$$\tau_B \approx \frac{\pi^2 e^2 h c}{(2\pi m_e c^3 T)^{1/2} m_e c^3} \approx \frac{\Delta L}{50 \text{cm}} \cdot \left(\frac{R}{10 \text{km}}\right)^{-1} \cdot \left(\frac{T}{35 \text{keV}}\right)^{-1/2} \quad (41)$$

This implies that if the line of sight covers 50cm or more of the source, radiative transfer will be important.

The preceding considerations apply if the infalling protons directly excite the line. If, however, the protons simply thermalize without yielding appreciable line emission, the problem becomes that of calculating a thermal production coefficient. Applying the results of such a calculation shown in Fig. 6 to the observation of Trümper et al. (1977 and 1978), we obtain the product of the density squared and the volume V of the source region

$$n^2 V \approx 2 \times 10^{56} \text{cm}^{-3} \quad (42)$$

for a temperature of 35 keV and field strength of 6×10^{12} G. As before, we can set an upper limit on the volume, and thus a lower limit on the density, by assuming that the transverse area occupied by the accreting matter is at most $\pi \cdot (0.1R)^2$, or

$$A \leq 3 \times 10^{10} \text{cm}^2 \left(\frac{R}{10 \text{km}}\right)^2 \quad (43)$$

This limit, together with that expressed by (39), implies

$$n \geq 3 \times 10^{20} \text{cm}^{-3} \left(\frac{R}{10 \text{km}}\right)^{-3} \quad (44)$$

so that transfer is important in this case, also. Therefore, an optically thin treatment of this radiation, as in Daugherty and Ventura (1977) is not likely to relate directly to observations.

We have considered the problem of line transfer in a rudimentary way, by calculating the opacity at a given angle and frequency for a thermal gas of electrons. The motivation for this is the following: where the opacity is large, photons are trapped in the source and must diffuse out, and at the surface, the intensity radiating outward approaches approximately its blackbody value. Therefore, where $\tau(\omega, \theta) \geq 1$, we assume the line rises out of the continuum. The best fit value of the width of the line reported by Trümper et al. (1977 and 1978) is ≤ 12 keV; as mentioned above, the field implied is $\sim 6 \times 10^{12}$ G, and in addition, they show evidence that this feature is produced in a gas with temperature ~ 35 keV. So for these conditions and four values of electron column density, we have estimated the width of a cyclotron line feature for several viewing angles by finding the frequencies where $\tau = 1$. Since Doppler shifting by the motion of the electrons is responsible for most of the smearing of the opacity, we expect the line to be narrowest at 90° to the field lines (and electron motion) and to broaden as the angle departs from this. Another factor which is important is the maximum frequency allowed, given by equation (29), especially near 90° , where it is responsible for the high energy drop in line opacity.

The results for the line width are shown in Figure 7, for viewing angles from 10° to 90° , and electron column densities 10^{22} , 10^{23} , 10^{24} , and 10^{25} cm^{-2} . As can be seen, for an electron temperature of 35 keV, this calculation cannot reproduce the width of the observed feature. The column density can't be much lower than 10^{22} cm^{-2} because of the

estimates of lower limits on the density expressed in equations (40) and (44). Thus to be consistent with the observation, we are forced to assume a lower electron temperature. As mentioned before, lower energy measurements have placed the temperature greater than 20 keV; so we have shown the line width results for this value also. Here we find that the reported width can be reproduced if the viewing angle is restricted to be very close to 90° and if the column density is the very minimum allowed. We note that the same conclusion about the viewing angle has been arrived at classically (Meszaros 1978). We also point out that the line of sight through the 20 keV source must be less than 100 cm. at most. Preliminary results from the A-4 experiment on HEAO-1, however, have indicated that if the emission above 40 keV is interpreted as a line feature, the best fit width is ~ 60 keV (the lower limit is ~ 18 keV, D. Gruber, private communication). From Figure 7, we see that the viewing angle is restricted to values greater than about 40° in this case, and the source column density can be increased considerably.

Interpretation of the > 40 keV X-radiation as cyclotron line emission doesn't explain the sudden steepening of the spectrum at around 20 keV (Pravdo et al., 1978). Boldt et al. (1976) proposed an isotropic Compton scattering as the cause; however, we have attempted to attribute this feature to an absorption edge or dip. As has been shown, cyclotron absorption can be treated as a resonance in the Compton process. A problem arises if the dip is due to cyclotron absorption, however, because of the high field strength implied ($> 2 \times 10^{12}$ G). If the absorbing electrons are located in such a high field, then they must be near the hard X-ray source. Consequently, they are bathed in X-rays and should be heated to a temperature approaching that of the source region itself. We have shown above that line transfer

is equivalent to scattering with a much smaller mean free path than Compton scattering. In this case, electrons near the source heated to temperatures near the source temperature become part of the very thick line scattering region. In other words, they re-emit the absorbed radiation in a manner similar to the source itself, and no absorption dip appears. The knock-ons discussed in the preceding section are a possible solution to this problem. These electrons stream down the field lines toward the stellar surface with $\beta \sim 0.6$ to 0.8, and can consequently absorb upward moving photons with frequencies less than the fundamental cyclotron frequency because of Doppler blue-shifting. Since the knock-ons are mildly relativistic, they preferentially reemit a line photon in their forward direction, i.e. downward toward the surface out of our viewing direction. If the column density of knock-ons is greater than unity, photons with high enough energies could be depleted in the same manner as for ionizing photons in an ionization bounded HII region. That is, photons Doppler shifted to cyclotron frequencies would be screened out by the knock-ons in the same way that hydrogen atoms screen ionizing photons.

The absorption depth of the knock-ons can be estimated by using the production rate expressed by equation (39) and by assuming that the fast electrons lose energy by absorbing upward photons and re-emitting them downward. We estimate the accretion rate by assuming an efficiency of 10% for the conversion of kinetic energy to X-radiation, and the cross-sectional area of $3 \times 10^{10} \text{ cm}^2$ for the accretion column. The lifetime is roughly given by the number of photon collisions required to

give up its energy (~ 10 for a 250 keV knock-on) divided by the collision frequency. The photon number density is obtained from the luminosity L_x , greater than 20 keV, by

$$n_x \approx \frac{L_x (> 20 \text{ keV})}{A c \langle \hbar \omega \rangle} \sim 4 \times 10^{21} \text{ cm}^{-3}, \quad (45)$$

assuming 1% of the total luminosity comes out above 20 keV. For infall energies of ~ 150 MeV/nucleon and $B = 6 \times 10^{12}$ G, equation (37) yields $N_{e,0} \approx \varphi_0$ and thus the absorption depth τ is estimated to be:

$$\tau_a = N_{e,0} \sigma_a T \sim \varphi_0 \sigma_a \frac{10}{n_x \sigma_a c} \sim 1 \quad (46)$$

for the assumptions given above. This value implies that knock-ons could be responsible for an absorption dip.

This picture also predicts a certain behavior of the absorption feature with pulse phase. In particular, as the line of sight comes closer to the polar field lines, the energy at which absorption begins should become lower, and the variation in energy should become smoother. In a recent paper (Pravdo et al., 1978), we assumed an arbitrary high energy electron distribution, and directly compared data from the cosmic X-ray experiment on OSO-8 with these predictions. As discussed there, the fit was acceptable over the region of the spectral pulse, and the best fit angles generally performed $\sim 20^\circ$ excursion in a region around 40° . As opposed to the line emission interpretation, however, here the spectral pulse (which may only be loosely correlated with the intensity pulse) defines a pencil beam

(or cone). The best fit field strength was coincidentally consistent with the emission measurements, $\sim 6 \times 10^{12}$ G. The cyclotron photon energies here are too broad to form a well-defined narrow line feature, but can be made consistent with the HEAO-1 A4 data.

V. Summary and Discussion

The strong magnetic fields ($\gtrsim 10^{12}$ G) believed to exist at the surfaces of neutron stars can strongly modify the interactions of electrons with ions and radiation. We have considered the effects of such modifications on the X-ray spectra of the pulsars in binary systems which derive their luminosity by accretion from their companions. The effect of the intense field is to quantize the allowed electron momenta transverse to the field lines. Radiative transitions between levels give rise to cyclotron emission and absorption, and since transverse momentum transfer from an ion to an electron must occur in discrete quanta, the Coulomb cross section becomes a knock-on cross section and a series of excitation cross sections. We have shown that electrons in the polar caps should almost always be found in their ground state and have then calculated the cross sections for these processes treating the electrons relativistically.

Since Hercules X-1 is the best studied of these binary X-ray pulsars and shows a possible line feature, we have used the above cross sections in an attempt to understand the physical conditions in the polar cap of this source. Data from 2 to ~ 20 keV imply that the effective electron temperature in the source is greater than 20 keV. To produce the observed line feature with a width (FWHM) less than 12 keV, we find

that the temperature cannot be higher than 20 keV, the angle between our line of sight and the polar cap field lines must lie within 10° of 90° during the entire high intensity part of the pulse, and the linear extent of the source along the line of sight must be less than 100cm. Recent measurements, however, relax these requirements considerably, allowing the viewing angle to be as low as $\sim 40^\circ$ and the line of sight to be much larger. Also, we have attempted to explain the spectral steepening at ~ 20 keV in terms of an absorption dip. The absorption dip can be made consistent with line observations because of the ability of the ions to produce a high parallel momentum population of knock-ons, which would absorb upward moving continuum photons and reemit them preferentially downward.

The observations required to determine the nature of the Her X-1 radiation, as well as that from similar sources, must include both spectral and temporal resolution. The OSO-8 observations of Her X-1 (Pravdo et al. 1977 and 1978) showed dramatic spectral changes below 30 keV over a portion of the pulse phase, and recent observations from the A-2 experiment on HEAO-1 (Pravdo et al. 1979) show evidence for pulse phase variations at higher energies. Generally pulse periods are \sim a second or longer, so time resolution on the order of tens of milliseconds is adequate. As for spectral resolution, we note the disagreement between scintillation spectrometers for the higher energy radiation, and point out that solid state devices could be made sensitive to energies as low as 40 keV with much improved resolution. Perhaps most importantly, an understanding of the variations already observed at lower energies with proportional counters may make clear the physical processes and conditions in such sources.

For helpful discussions, I would like to thank Drs. Steven Pravdo, Reuven Ramaty, Elihu Boldt, Barham Smith, and Joseph Daugherty. Also, Dr. S. Langer is gratefully acknowledged for an important correction. The research was supported by NASA grant NGR 21-002-316.

REFERENCES

Abramowitz, B. and Stegun, I. A. 1965, *Handbook of Mathematical Functions* (New York: Dover).

Barashenkov, V. S. and Maltsev, V. M. 1961, *Fortschritte der Physik*, 9, 549.

Basko, M. M. and Sunyaev, R. A. 1975, *Astron. and Astrophys.*, 42, 311.

Bjorken, J. D. and Drell, S. D. 1964, *Relativistic Quantum Mechanics* (New York: McGraw-Hill).

Boldt, E. A., Holt, S. S., Rothschild, R. E., and Serlemitsos, P. J. 1976, *Astron. and Astrophys.* 50, 161.

Book, D. L. and Ali, A. W. 1975, *A Collection of Plasma Physics Formulas and Data*, NRL Memorandum Report 2898.

Canuto, V., Lodenquai, J., and Ruderman, M. 1971, *Phys. Rev. D*, 3, 2303.

Canuto, V. and Ventura, J. 1977, *Fundamentals of Cosmic Physics*, 2, 203.

Catura, R. C., and Acton, L. W. 1975, *Ap. J. Letters*, 202, L5.

Coe, M. J., Engel, A. R., Quenby, J. J., and Dyer, C. S. 1977, *Nature*, 268, 508.

Danese, A. E. 1965, *Advanced Calculus*, Vol. I (Boston: Allyn and Bacon).

Daugherty, J. K., and Ventura, J. 1977, *Astron. and Astrophys.*, 61, 723.

Daugherty, J. K., and Ventura, J. 1978, *Phys. Rev. D*, 18, 1053.

Giacconi, R., Gursky, H., Kellogg, E., Levinson, R., Schreier, E., and Tananbaum, H. 1973, *Ap. J.*, 184, 227.

Lee, J. F. 1979, preprint.

Merzbacher, E. 1970, *Quantum Mechanics* (New York: Wiley).

Meszaros, P. 1978, preprint.

Pravdo, S. H., Boldt, E. A., Holt, S. S. and Serlemitsos, P. J. 1977, *Ap. J. Letters*, 216, L23.

Pravdo, S. H., Bussard, R. W., Becker, R. H., Boldt, E. A., Holt, S. S.,
Serlemitsos, P. J. and Swank, J. H., Ap. J., 225, 988.

Pravdo, S. H., Bussard, R. W., and White, N. E. 1979, M.N.R.A.S., in press.

Schulman, S., Friedman, H., Fritz, G., Henry, R. C., and Yentis, D. J.
1975, Ap. J. Letters, 119, L101.

Trumper, J., Pietsch, W., Reppin, C., Sacco, B., Kendziorra, E., and
Staubert, R. 1977, Texas Symp. on Relativistic Astrophys. (Boston, 1976),
ann. N.Y. Acad. Sci., in press.

Trumper, J., Pietsch, W., Reppin, C., Voges, W., Staubert, R., and
Kendziorra, E. 1978, Ap. J. Letters, 219, L105.

Ventura, J. 1973, Phys. Rev. A, 8, 3021.

Figure Captions

Figure 1 - The radiative lifetime of the first excited magnetic state as a function of field strength, for both Landau ($s=-\frac{1}{2}$) and spin ($s=+\frac{1}{2}$) excitations.

Figure 2 - The Coulomb cross sections for excitation and knock-on collisions in fields of 10^{12} and 6×10^{12} G as a function of the electron energy in the proton rest frame or vice versa. The electrons are initially in the ground state and the ions have zero pitch angle; j labels the final transverse momentum state.

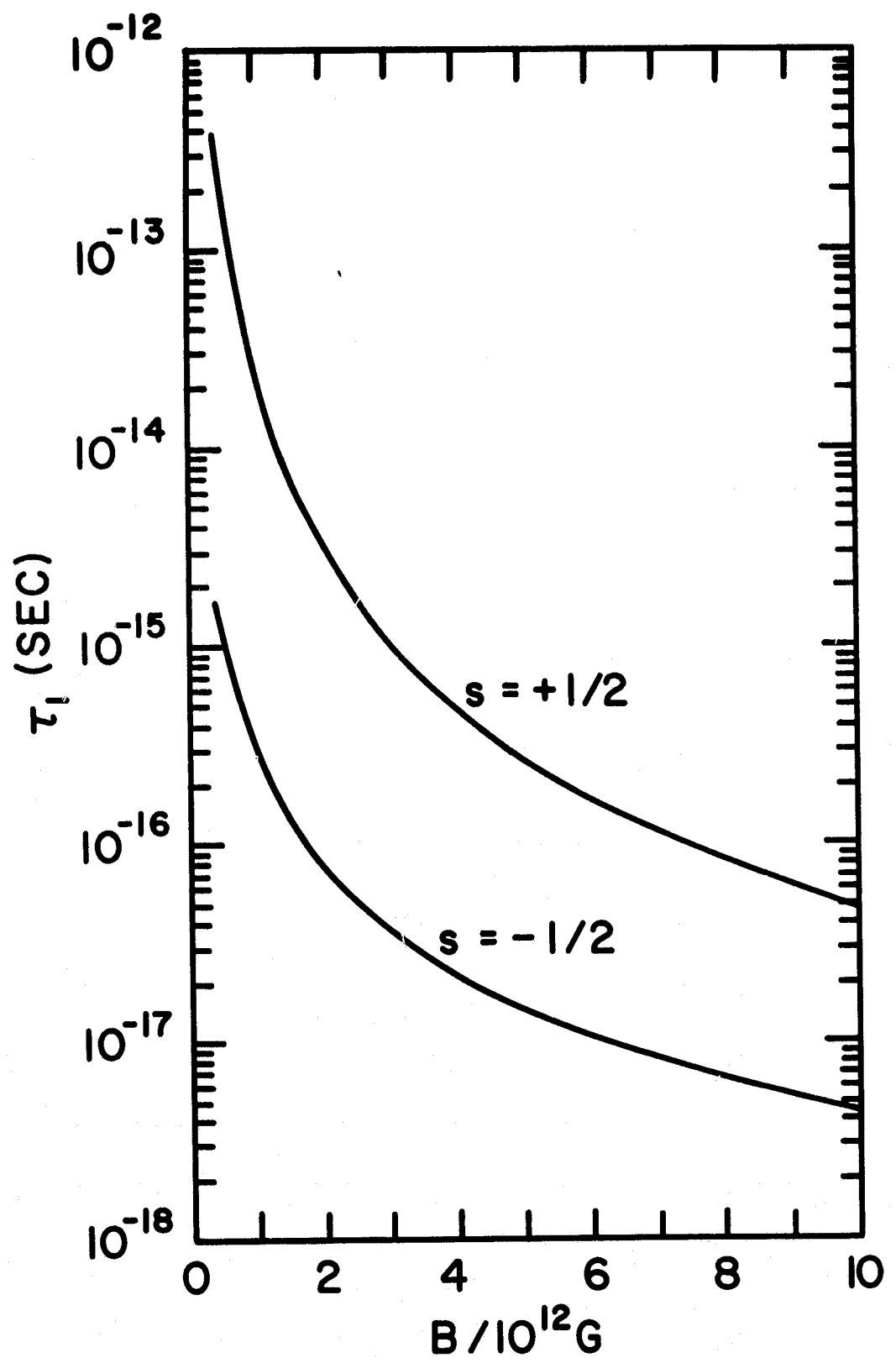
Figure 3 - The Coulomb energy losses suffered by zero pitch angle protons per unit matter traversed for several temperatures in a field of 6×10^{12} G as a function of the proton energy. Also shown are the losses in a non-magnetized gas with $kT = 35$ keV and in a field of 10^{12} G with $kT = 15$ keV.

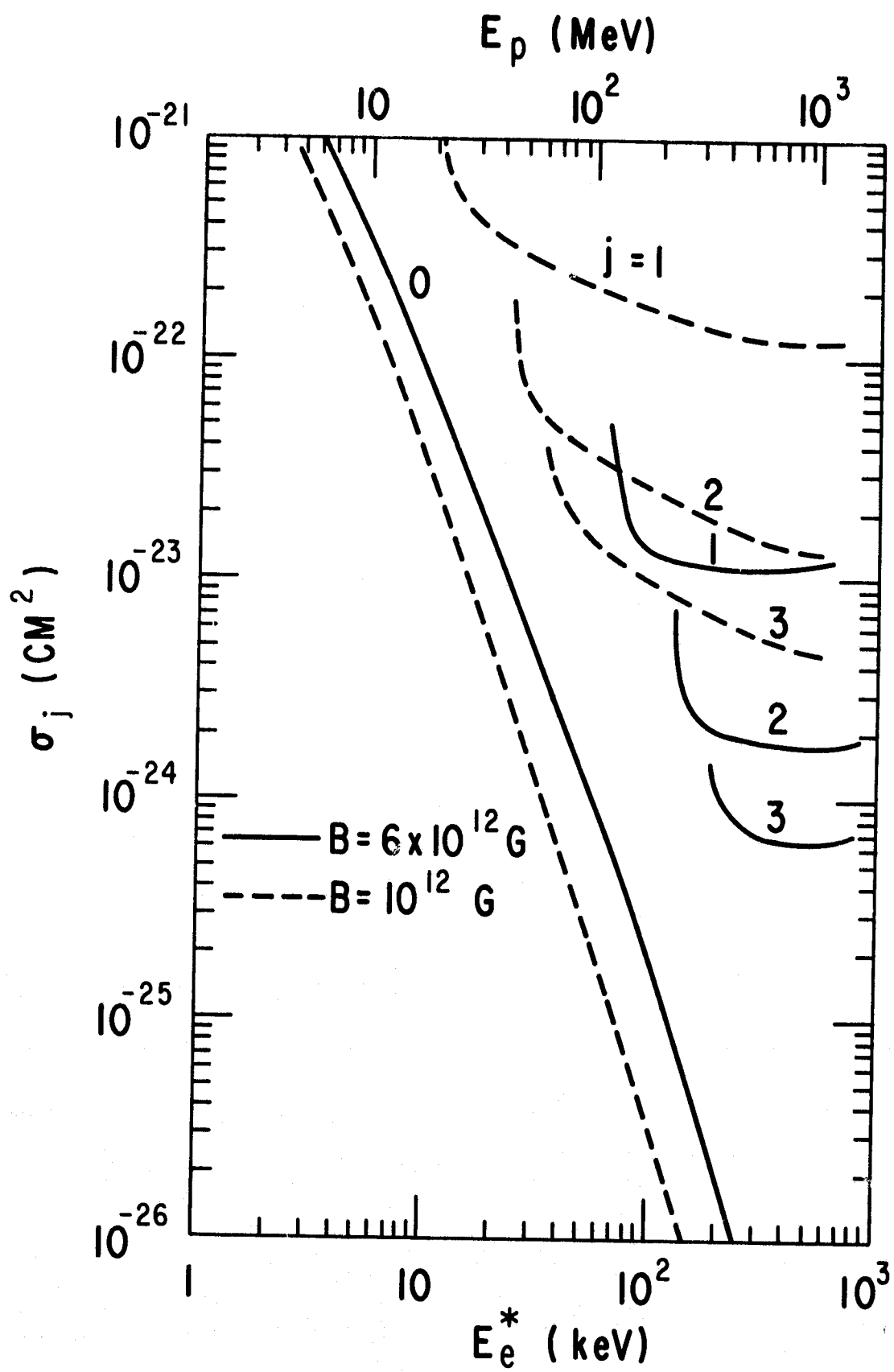
Figure 4 - The Coulomb range of zero pitch angle protons, neglecting nuclear encounters, in gases at several temperature and $B = 6 \times 10^{12}$ G.

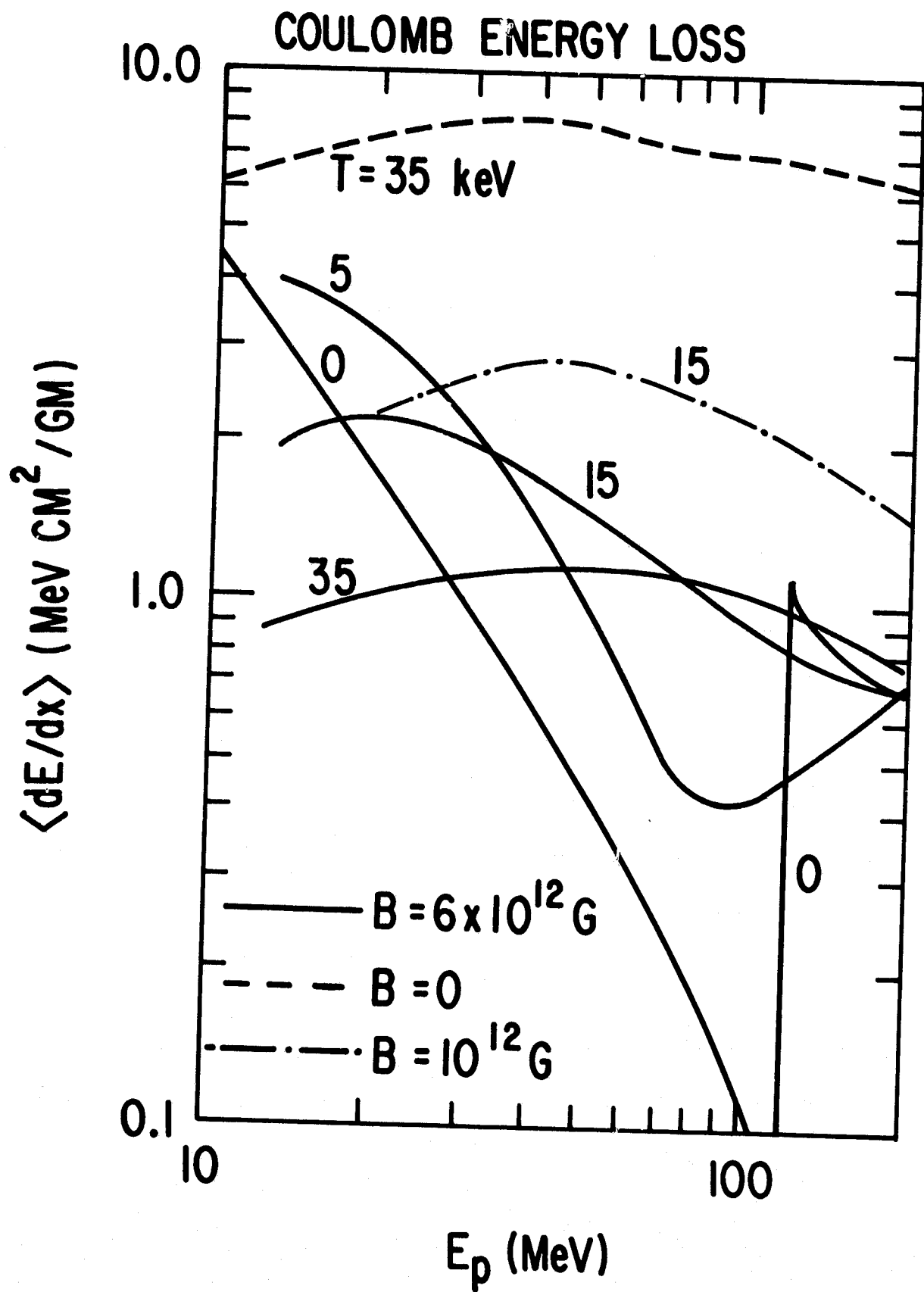
Figure 5 - a) The multiplicity of line photons produced as a result of Coulomb interactions with infalling protons as a function of the initial energy of the proton.
b) The fraction of the proton kinetic energy going into line radiation.

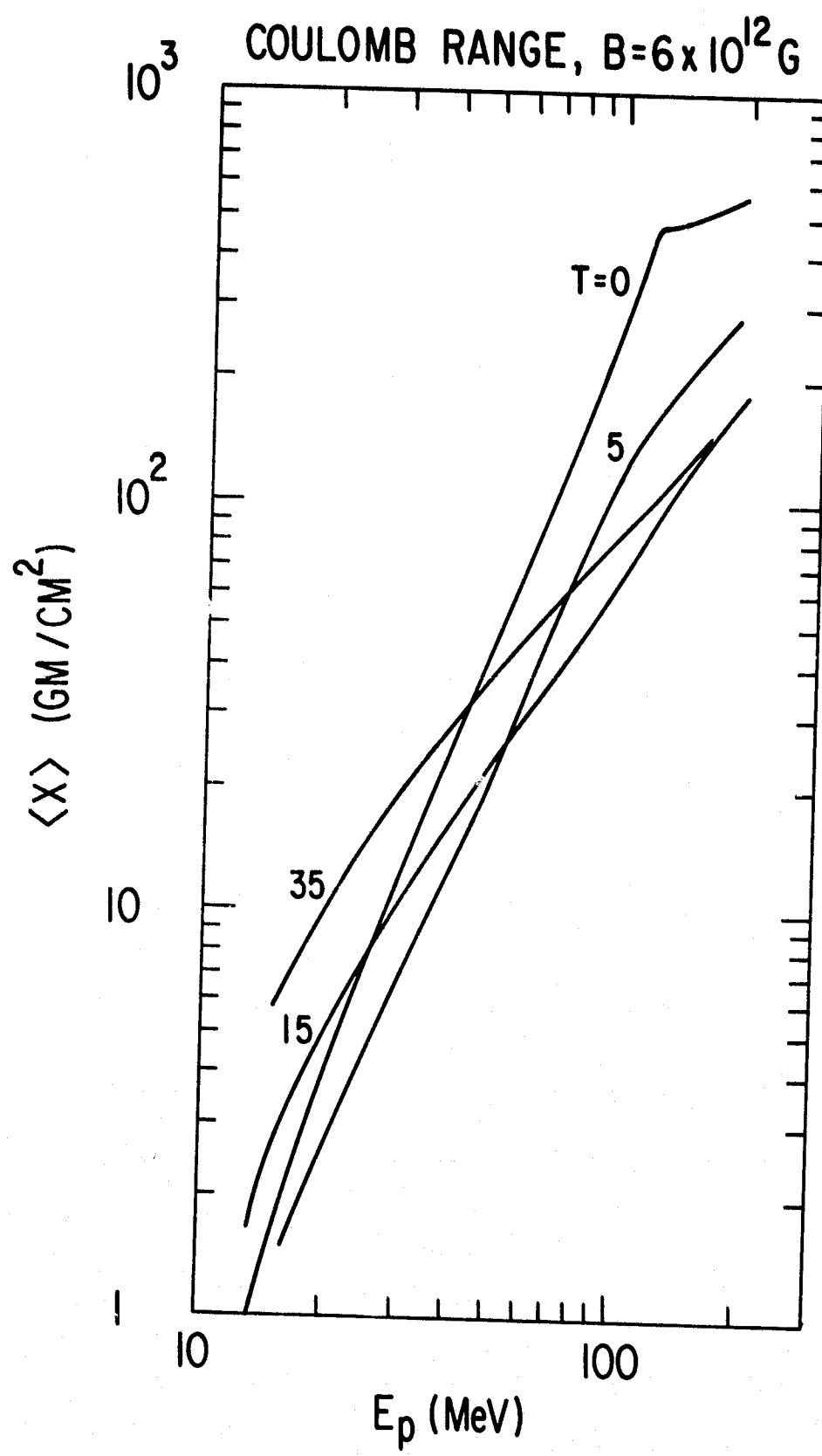
Figure 6 - The coefficient for thermal excitation of the first excited state in fields of 1 and 6×10^{12} G as functions of the gas temperature.

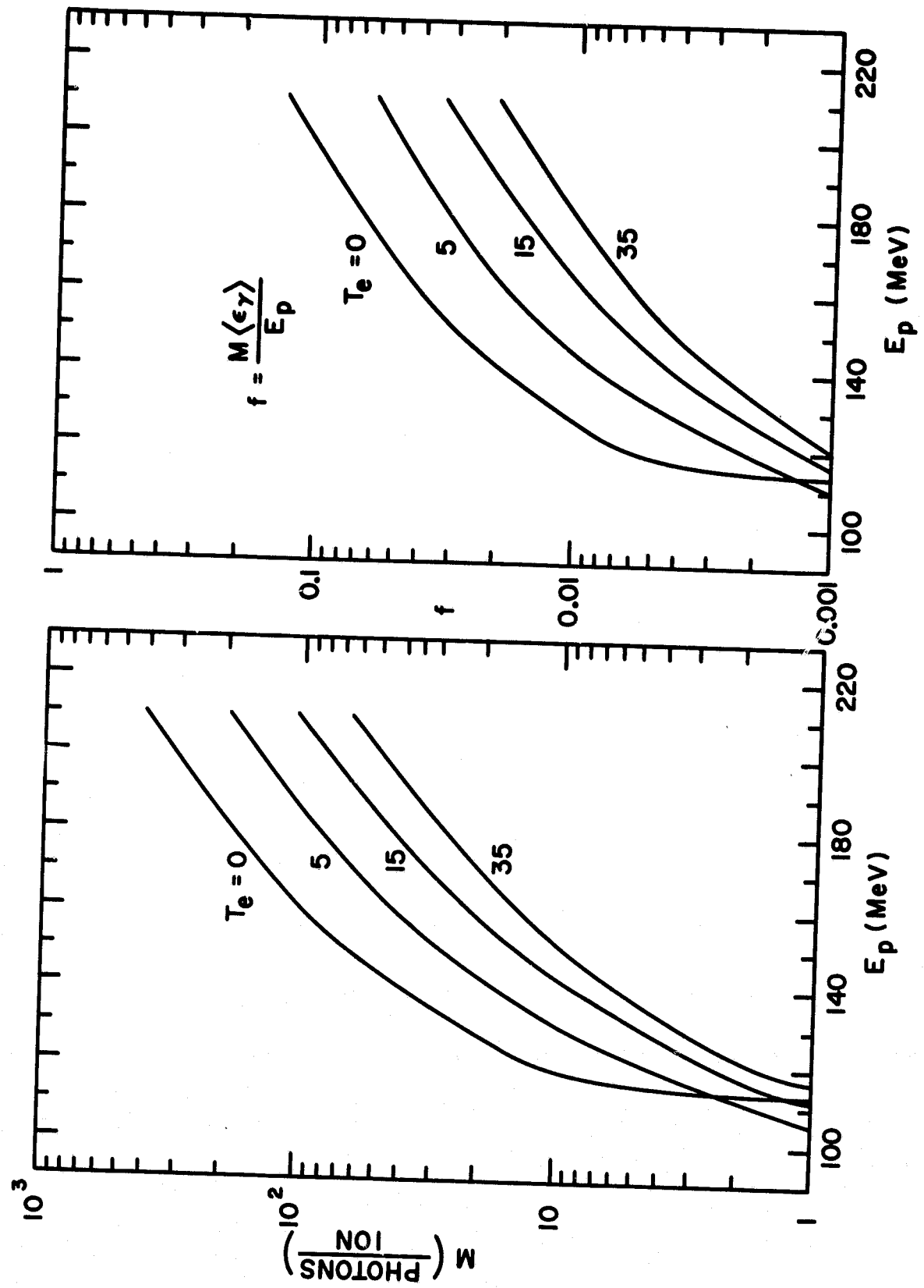
Figure 7 - The width of the fundamental cyclotron line determined from opacity (self-absorption) for two temperatures and four values of column density for the source electrons.

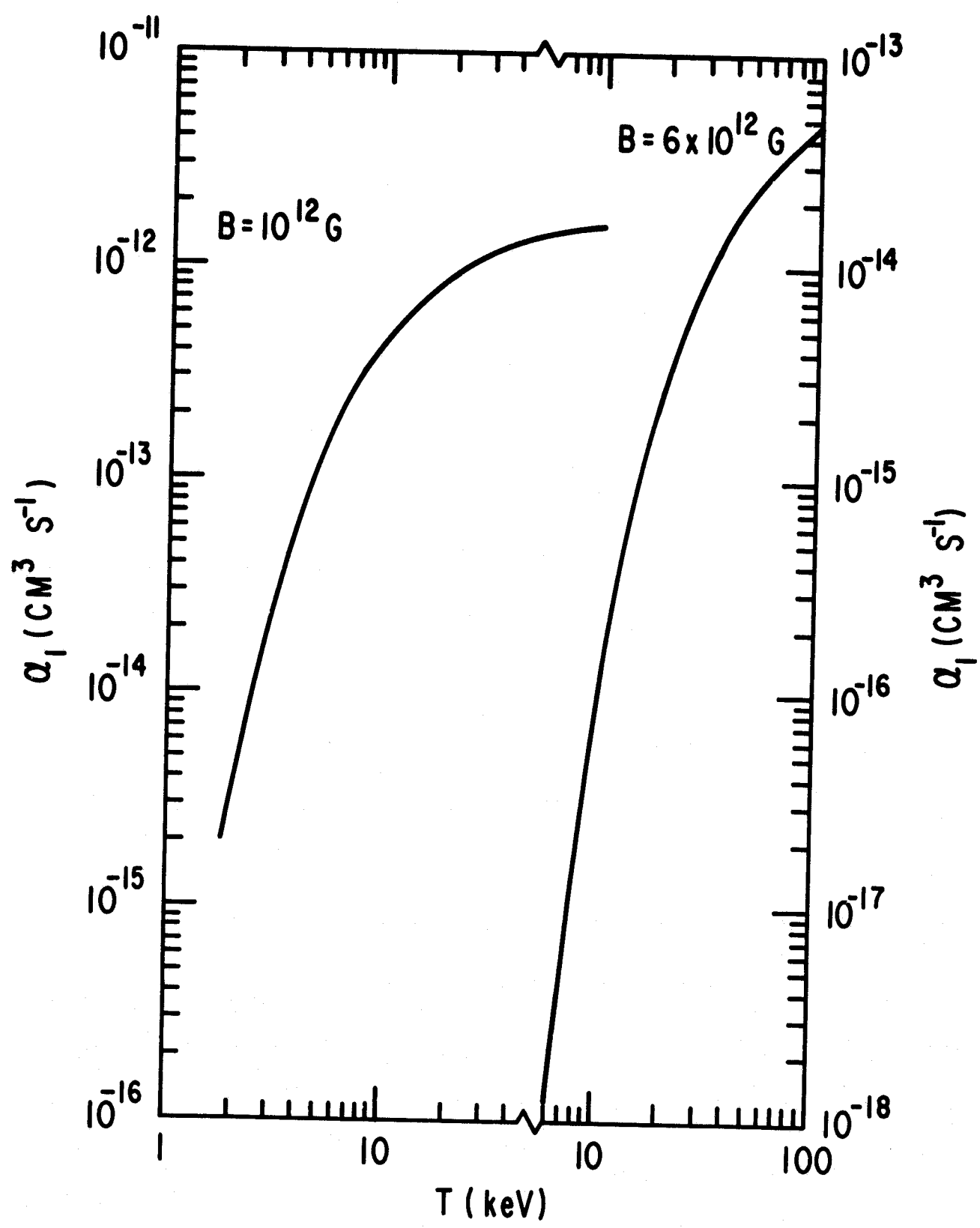


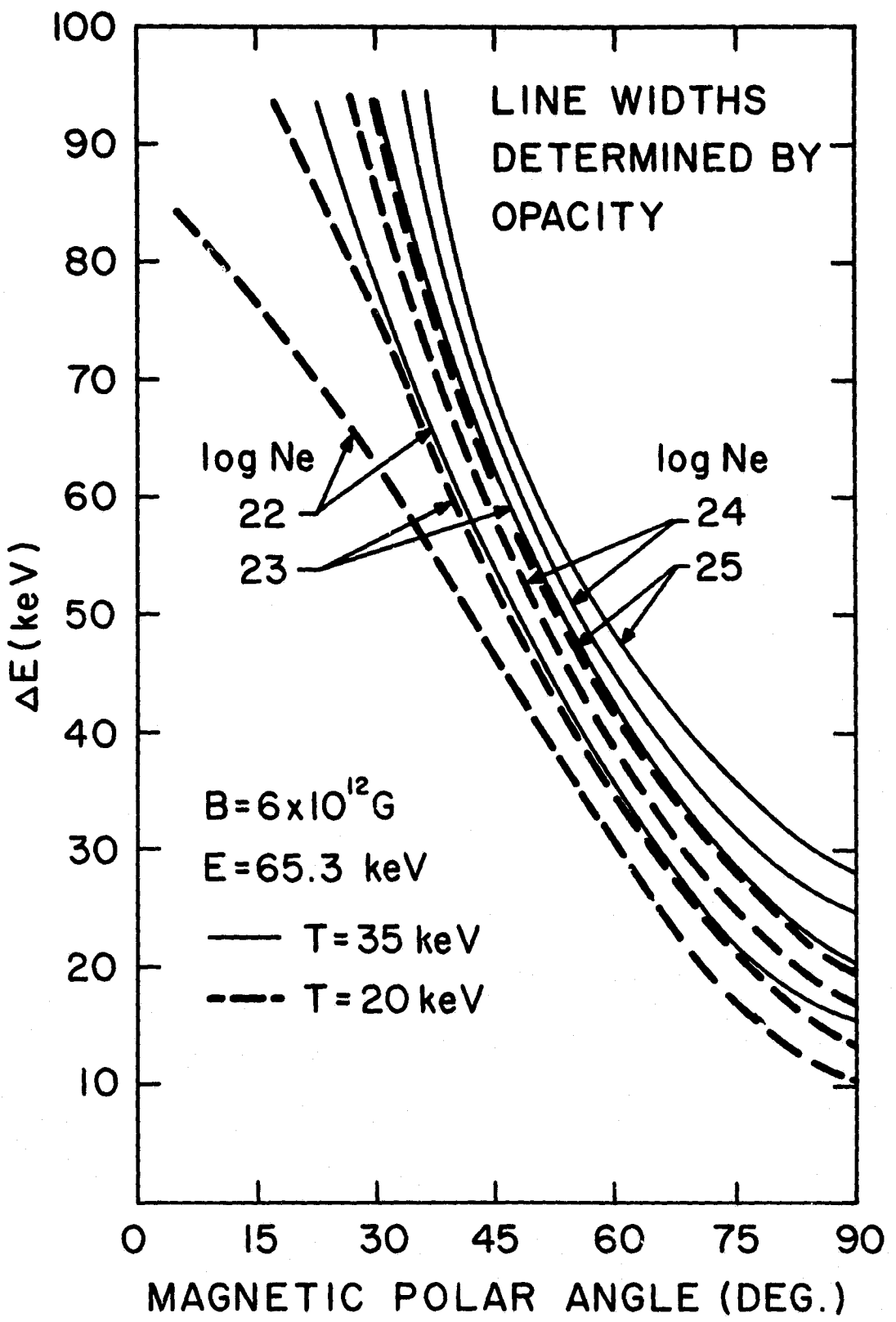












APPENDIX

In this appendix, we present the details of the calculations of the cross sections and emission rates presented in this paper. First we evaluate an integral occurring in all the calculations:

$$I_{n_1, q_1; n_2, q_2}(\vec{k}_\perp) = \int d^2 x_\perp f_{n_1, q_1}^*(\vec{x}_\perp) \exp(i \vec{k}_\perp \cdot \vec{x}_\perp) f_{n_2, q_2}(\vec{x}_\perp) \quad (A1)$$

in an operator representation. The argument of the exponential can be written using equation (8),

$$i \vec{k}_\perp \cdot \vec{x}_\perp = i (k^+ x^- + k^- x^+) = i k^+ (X^- + \frac{i}{eB} \pi^-) + i k^- (X^+ - \frac{i}{eB} \pi^+) \quad (A2)$$

where a vector \vec{v} is decomposed according to

$$v^\pm = 2^{-\frac{1}{2}} (v^* \pm i v^\gamma) \quad (A3)$$

The commutation relations among the various operators are as follows:

$$\begin{aligned} [\pi^+, \pi^-]_- &= -eB \\ [X^+, X^-]_- &= \frac{1}{eB} \\ [\pi^\pm, X^\pm]_- &= 0 \end{aligned} \quad (A4)$$

From Merzbacher, (1970, p. 167) we obtain for this situation:

$$\exp(A_1 + A_2) = \exp(A_1) \cdot \exp(A_2) \cdot \exp(-\frac{1}{2} [A_1, A_2]_-) \quad (A5)$$

Applying this relation to the exponential in A-1 gives:

$$\exp(i \vec{k}_\perp \cdot \vec{x}_\perp) = \exp(i k^+ X^-) \exp(i k^- X^+) \exp(\frac{k^- \pi^+}{eB}) \exp(-\frac{k^+ \pi^-}{eB}) e^{-\xi} \quad (A6)$$

where $\xi = k_\perp^2 / (2eB)$. Thus, substituting in A-2 and using the hermiticity of

the operators, $(X^-)^\dagger = X^+$; $(\pi^-)^\dagger = \pi^+$, yields

$$I_{n_1, q_1; n_2, q_2} = e^{-\frac{s}{2}} \int d^2 x_L \left[\exp(-i k^- X^+) \exp\left(\frac{k^+}{2B} \pi^-\right) f_{n_1, q_1} \right]^\dagger \cdot \exp(i k^- X^+) \exp\left(-\frac{k^+}{2B} \pi^-\right) f_{n_2, q_2} . \quad (A7)$$

Expanding the exponential and operating on the functions according to equations (9) and (10) gives

$$I_{n_1, q_1; n_2, q_2} = e^{-\frac{s}{2}} \int d^2 x_L \left[\sum_{\eta_1=0}^{n_1} \sum_{\mu_1=0}^{q_1} \frac{(-i k^-)^{\mu_1}}{\mu_1!} \frac{(k^+)^{\eta_1}}{\eta_1!} (2B)^{-\frac{\mu_1+\eta_1}{2}} f_{n_1-\eta_1, q_1-\mu_1} \right]^* \quad (A8)$$

$$\cdot \sum_{\eta_2=0}^{n_2} \sum_{\mu_2=0}^{q_2} \left[\frac{n_1!}{(n_1-\eta_1)!} \frac{n_2!}{(n_2-\eta_2)!} \frac{q_1!}{(q_1-\mu_1)!} \frac{q_2!}{(q_2-\mu_2)!} \right]^{\frac{1}{2}} \frac{(-i k^-)^{\mu_2}}{\mu_2!} \frac{(-k^+)^{\eta_2}}{\eta_2!} (2B)^{-\frac{\mu_2+\eta_2}{2}} f_{n_2-\eta_2, q_2-\mu_2} ,$$

which yields after using the orthogonality property of the f 's and

$k^\pm = k_L e^{\pm i \frac{\pi}{2}/2}$, where ω is the azimuth of \vec{k} in the transverse plane,

$$I_{n_1, q_1; n_2, q_2} = e^{-\frac{s}{2}} i^{(q_1-q_2)} (-1)^{n_2-n_1} (n_1! n_2! q_1! q_2!)^{\frac{1}{2}} \cdot \sum_{\eta_1=\max(0, n_1-n_2)}^{n_1} \sum_{\mu_1=\max(0, q_1-q_2)}^{q_1} \frac{(\sqrt{s})^{n_2-\eta_1+q_2-q_1}}{\mu_1! \eta_1! (n_2-n_1+\eta_1)! (q_2-q_1+\mu_1)! (n_1-\eta_1)! (q_1-\mu_1)!} e^{i(n_2-n_1-q_2+q_1)\varphi} \quad (A9)$$

Substituting $\eta_1 = \eta_1 - \max(0, n_1-n_2)$ and $\mu_1 = \max(0, q_1-q_2)$ yields

$$I_{n_1, q_1; n_2, q_2} = e^{-\frac{s}{2}} i^{(1_{q_1-q_2} + 1_{n_2-n_1} + n_2-n_1)} \cdot (n_1! n_2! q_1! q_2!)^{\frac{1}{2}} (\sqrt{s})^{1_{n_2-n_1} + 1_{q_2-q_1}} \cdot e^{i(n_2-n_1-q_2+q_1)\varphi} \cdot \sum_{\eta=0}^{\min(n_1)} \sum_{\mu=0}^{\min(q_1)} \frac{(-\frac{s}{2})^{\mu+\eta}}{\mu! \eta! (\mu+1_{q_2-q_1})! (n_1+\min(n_1, n_2)-\eta)! [\min(n_1, n_2)-\eta]! [\min(q_1, q_2)-\mu]} \quad (A10)$$

From the definition of the Laguerre polynominal:

$$L_s^{(\alpha)}(x) = \sum_{m=0}^s \frac{\Gamma(s+\alpha+1)}{(s-m)! \Gamma(m+\alpha+1)} \frac{(-x)^m}{m!} \quad (A11)$$

we see that (A-10) can be written

$$I_{n_1, q_1; n_2, q_2} = e^{-\frac{s}{2}} i^{(1_{q_1-q_2} + 1_{n_2-n_1} + n_2-n_1)} \left[\frac{\min(n_1, n_2)! \min(q_1, q_2)!}{\max(n_1, n_2)! \max(q_1, q_2)!} \right]^{\frac{1}{2}} (\sqrt{s})^{1_{n_2-n_1} + 1_{q_2-q_1}} e^{i(n_2-n_1-q_2+q_1)\varphi} L_{\min(n_1, n_2)}^{(1_{n_2-n_1})}(\frac{s}{2}) L_{\min(q_1, q_2)}^{(1_{q_2-q_1})}(\frac{s}{2}) \quad (A12)$$

We can now proceed to the evaluation of the cross sections.

First we calculate the absorption cross section and emission rate for line photons as prescribed by equations (13) and (14):

$$S_{fi} = ie \left(\frac{2\pi}{\omega \gamma} \right)^{1/2} \int d^4x \bar{\psi}_f(x) \vec{\gamma} \cdot \hat{\epsilon} e^{-i(\omega t - \vec{k} \cdot \vec{x})} \psi_i(x), \quad (A-13)$$

for absorption. Substitution from equation (6) for ψ gives

$$S_{fi} = \frac{ie}{2L} \left[\frac{2\pi}{\omega \gamma \omega_f \omega_i (m_f + m_e) (m_i + m_e)} \right]^{1/2} \int d^4x \left[(\gamma^\mu \pi_\mu + m_e) f_{n_f, g_f}(\vec{x}_f) e^{-i(\omega_f t - p_f \cdot \vec{x}_f)} u_{s_f} \right]^+ \gamma^\nu \vec{\gamma} \cdot \hat{\epsilon} e^{-i(\omega t - \vec{k} \cdot \vec{x})} (\gamma^\nu \pi_\nu + m_e) f_{n_i, g_i}(\vec{x}_i) e^{-i(\omega_i t - p_i \cdot \vec{x}_i)} u_{s_i}, \quad (A-14)$$

which, after using the hermiticity of the Dirac matrices ($\gamma^\mu = \gamma^0 \gamma^1 \gamma^2 \gamma^3$).

$$S_{fi} = \frac{ie}{2L} \left[\frac{2\pi}{\omega \gamma \omega_f \omega_i (m_f + m_e) (m_i + m_e)} \right]^{1/2} \int d^4x f_{n_f, g_f}^*(\vec{x}_f) e^{i(\omega_f t - p_f \cdot \vec{x}_f)} u_{s_f}^+ \gamma^\nu (\gamma^\mu \pi_\mu + m_e) \vec{\gamma} \cdot \hat{\epsilon} e^{-i(\omega t - \vec{k} \cdot \vec{x})} (\gamma^\nu \pi_\nu + m_e) u_{s_i} f_{n_i, g_i}(\vec{x}_i) e^{-i(\omega_i t - p_i \cdot \vec{x}_i)}. \quad (A-15)$$

This expression can be reduced to 2×2 from 4×4 by using

$$u_s = \begin{pmatrix} 1 & s \\ 0 & 0 \end{pmatrix}, \quad \gamma^0 = \begin{pmatrix} 1 & 0 \\ 0 & -1 \end{pmatrix}, \quad \vec{\gamma} = \begin{pmatrix} 0 & \vec{\sigma} \\ -\vec{\sigma} & 0 \end{pmatrix} \quad (A-16)$$

where $|s> = \begin{pmatrix} \delta_{s,1} & \frac{1}{2} \\ \delta_{s,-1} & -\frac{1}{2} \end{pmatrix}$ and $\vec{\sigma}$ are the Pauli matrices. After commuting the exponential factor to the left, we obtain the matrix operator between states

$$\begin{aligned} & \gamma^0 [\gamma^\mu (\pi_\mu + k_\mu) + m_e] \vec{\gamma} \cdot \hat{\epsilon} (\gamma^\nu \pi_\nu + m_e) \\ &= \left((\pi_0 + \omega + m_e) (\vec{\epsilon} \cdot \vec{\pi} + i \vec{\sigma} \cdot \hat{\epsilon} \times \vec{\pi}) + (\pi_0 + m_e) [\vec{\epsilon} \cdot \vec{\pi} + i \vec{\sigma} \cdot (\vec{\pi} + \vec{k}) \times \hat{\epsilon}] \right. \\ & \quad \left. - \right) \end{aligned} \quad (A-17)$$

where some components are not shown because they are not needed. Then

ORIGINAL PAGE IS
OF POOR QUALITY

the matrix element A-15 becomes

$$S_{fi} = \frac{ie}{2L} \left[\frac{2\pi}{\omega V w_f w_i (w_f + m_e) (w_i + m_e)} \right]^{1/2} \int d^4x f_{n_f, q_f}^*(\vec{x}_+) e^{i(w_f t - p_f \cdot \vec{x}) - i(\omega t - \vec{k} \cdot \vec{x})} \\ \langle s_f | [(2\pi + 2m_e + \omega) \vec{\epsilon} \cdot \vec{\pi} + i\omega \vec{\sigma} \cdot \vec{\epsilon} \times \vec{\pi} + i(\pi_0 + m_e) \vec{\sigma} \cdot \vec{k} \times \vec{\epsilon}] | s_i \rangle f_{n_i, q_i}(\vec{x}_+) e^{-i(w_i t - p_i \cdot \vec{x})}$$

This equation is valid for all transitions between levels. We simplify by requiring that the initial state be the ground state, by letting $q_i = 0$ without loss of generality, and by evaluating in the center of parallel momentum frame, where $p_f = 0$ and $w_f = w_1 \equiv \sqrt{m^2 + 2eB}$. Under these conditions, equation A-18 becomes

$$S_{fi} = \left(\frac{ie}{2L} \right) \frac{(2\pi)^{5/2} \delta(w_i + \omega - w_1) \delta(p_f)}{[\omega V w_i w_1 (w_i + m_e) (w_1 + m_e)]^{1/2}} \left\{ \delta_{s_f, \pm \frac{1}{2}} [(2w_i + 2m_e + \omega) \vec{\epsilon}^3 \cdot \vec{p}_i - \right. \\ \left. (w_i + m_e) (\vec{k} \cdot \vec{\epsilon}^+ - \vec{k}^+ \cdot \vec{\epsilon}^-)] I_{1, q_f; 0, 0}(\vec{k}_\perp) + \delta_{s_f, \pm \frac{1}{2}} \frac{2\sqrt{2B}}{(w_i + m_e) \epsilon^0} I_{1, q_f; 1, 0}(\vec{k}_\perp) \right. \\ \left. + \delta_{s_f, \pm \frac{1}{2}} \sqrt{2} [(w_i + m_e) (\vec{k} \cdot \vec{\epsilon}^- - \vec{k}^- \cdot \vec{\epsilon}^3) - \omega \vec{p}_i \cdot \vec{\epsilon}^-] I_{0, q_f; 0, 0}(\vec{k}_\perp) \right\} \quad (A-19)$$

We note that if θ is the polar angle of \vec{k} and φ its azimuth,

$$\vec{\epsilon}^3 = -\epsilon_0 \sin \theta, \quad \vec{\epsilon}^\pm = \frac{1}{\sqrt{2}} e^{\pm i\varphi} (\epsilon_0 \cos \theta \mp i\epsilon_x) \quad (A-20)$$

where ϵ_0 and ϵ_x are the polarization amplitudes in the ordinary and extraordinary modes. Substituting for the I 's from A-12 gives

$$S_{fi} = -\frac{ie}{2L} \left[\frac{(2\pi)^{5/2} \delta(w_i + \omega - w_1) \delta(p_f)}{[\omega V w_i w_1 (w_i + m_e) (w_1 + m_e)]^{1/2}} \right] e^{-\vec{s} \cdot i\varphi} \frac{(i\sqrt{s} e^{i\varphi})^{8f}}{\sqrt{8_f!}} \left\{ \delta_{s_f, \pm \frac{1}{2}} \frac{\sqrt{2eB}}{(w_i + m_e + \omega \cos^2 \theta) \epsilon_0} \right. \\ \left. [(w_i + m_e + \omega) \vec{s} \cos \theta \epsilon_0 + (w_i + m_e) (\cos \theta \epsilon_0 + i\epsilon_x)] + \delta_{s_f, \pm \frac{1}{2}} \omega [(w_i + m_e + \omega \cos^2 \theta) \epsilon_0 \right. \\ \left. + i(w_i + m_e) \cos \theta \epsilon_x] \right\} \quad (A-21)$$

Carrying out the same analysis for the emission case gives (assuming

$$p_i, q_i = 0$$

$$S_{fi}(\text{emis}) = -\frac{ie}{2L} \frac{(i\pi)^{5/2} \delta(w_i - w - w_f) \delta(p_f + k^3)}{[\omega V w_i (w_i + m_e) w_f (w_f + m_e)]^{1/2}} e^{-s + i\varphi} \frac{(-i\sqrt{3} e^{i\varphi})^{q_f}}{\sqrt{q_f!}} \quad (A22)$$

$$\left\{ \delta_{s_i, \pm \frac{1}{2}} \sqrt{2e3} [(w_i + m_e) \pm \cos \theta \epsilon_0 + (w_f + m_e) (\cos \theta \epsilon_0 + i \epsilon_x)] + \delta_{s_i, \frac{1}{2}} \omega [(w_f + m_e + \omega \cos^2 \theta) \epsilon_0 + i (w_i + m_e) \cos \theta \epsilon_x] \right\}.$$

The absorption cross section is obtained by squaring the magnitude of S_{fi} and summing over electron final states. The square of the δ -functions are handled heuristically in Bjorken and Drell (1964):

$$|\delta(p)|^2 = \frac{L}{2\pi} \delta(p) , \quad |\delta(w)|^2 = \frac{T}{2\pi} \delta(w) , \quad (A23)$$

where L and T are the (large) normalization length parallel to the field and the normalization time. Then the rate of absorption is

$$\frac{1}{V} \sigma_a v_{\text{rel}} = \frac{1}{T} \frac{L}{2\pi} \int dp_f \sum_{q_f=0}^{\infty} |S_{fi}|^2 \quad (A24)$$

where V is the electron normalization volume, σ_a is the absorption cross section, and v_{rel} is the relative velocity of the photon and electron. Solving for the absorption cross section yields equation (15) in the center of parallel momentum frame.

The emission rate is shown in here in more detail to show the processes involved in arriving at equation (15). First, the sum over q_f yields

$$\sum_{q_f=0}^{\infty} \left| e^{-s} \frac{(-i\sqrt{3} e^{i\varphi})^{q_f}}{\sqrt{q_f!}} \right|^2 = e^{-s} \quad (A25)$$

The integral over p_f is ignored because of the δ function. The the emission rate into d^3k centered on k for electrons deexciting from

the first excited state can be written as

$$R_{01}(\vec{k}, \hat{\epsilon}) d^3k = \frac{V d^3k}{(2\pi)^3} \frac{1}{\pi} \int \frac{L d\beta_f}{2\pi} \sum_{\vec{p}_f} |S_{f1}|^2, \quad (A-26)$$

where $V d^3k / (2\pi)^3$ expresses the proportionality of the rate to the phase space volume for the emitted photon. Carrying out the operations yields

$$R_{01}(\vec{k}, \hat{\epsilon}) = \frac{e^2}{8\pi} \frac{\delta(\omega_f + \omega - \omega_i) 2eB e^{-\theta}}{\omega \omega_f \omega_i (\omega_f + m_e)(\omega_i + m_e)} \left\{ \delta_{s_{i1}, -\frac{1}{2}} [(\omega_i + m_e)\xi + \omega_f + m_e]^2 \right. \\ \left. \cos^2 \theta \xi_e^2 + \delta_{s_{i1}, \frac{1}{2}} (\omega_f + m_e)^2 \xi_x^2 + \delta_{s_{i1}, \frac{1}{2}} \frac{\omega^2}{2eB} [(\omega_i + m_e + \omega \cos^2 \theta)^2 \xi_e^2 \right. \\ \left. + (\omega_i + m_e)^2 \cos^2 \theta \xi_x^2] \right\} \quad (A-27)$$

When carrying out the integral over d^3k to obtain the inverse of the lifetime τ_1 , it must be noted that ω_f depends on ω so that the δ function in A-27 should be written

$$\delta(\omega_f + \omega - \omega_i) = \frac{\omega_f}{\omega_f + \omega \cos^2 \theta} \delta\left(\omega - \frac{\omega_i - \sqrt{\omega_i^2 \cos^2 \theta + m_e^2 \sin^2 \theta}}{\sin^2 \theta}\right). \quad (A-28)$$

Then we obtain

$$\tau_1^{-1} = \frac{e^2}{4} \int_{-1}^1 d\mu \frac{2eB \omega e^{-\theta}}{(\omega_f + \omega \mu^2)(\omega_i + m_e)(\omega_f + m_e)\omega_i} \left\{ \quad \right\} \quad (A-29)$$

where the braces represent the quantity in braces in A-27. This integral was evaluated numerically; the results are shown in Figure 1. When the radiative lifetime of an electron in the first excited state is short compared to collisional timescales, we can combine the absorption

and emission processes into a scattering cross section, given by

$$\frac{d\sigma(\omega, \mu)}{d\mu'} = \frac{\pi^2 e^4}{4} \frac{\omega'}{\omega} \frac{\delta(\omega - \frac{W_i - \sqrt{W_i^2 \mu^2 + m_e^2 \sin^2 \theta}}{1 - \mu^2}) \cdot (W_i - \omega) (m_e^2 + 2W_i \omega \mu^2)^{-\frac{1}{2}} e^{-(S+S')} }{W_i^2 (W_i + m_e)^2 (W_i + m_e - \omega) (W_i + m_e - \omega') (m_e^2 + 2eB \mu^2)^{-\frac{1}{2}} (m_e^2 + 2eB \mu'^2)^{-\frac{1}{2}}} \\ \left\{ (2eB)^2 \tau_i(-\frac{1}{2}) \left[((W_i + m_e)S + W_i + m_e - \omega)^2 \varepsilon_0^2 \mu^2 + (W_i + m_e - \omega)^2 \varepsilon_x^2 \right] \cdot \left[((W_i + m_e)S' + W_i + m_e - \omega')^2 \varepsilon_0'^2 \mu'^2 \right. \right. \\ \left. \left. + (W_i + m_e - \omega')^2 \varepsilon_x'^2 \right] + \omega^2 \omega'^2 \tau_i(\frac{1}{2}) \left[(W_i + m_e - \omega \sin^2 \theta)^2 \varepsilon_0^2 + (W_i + m_e)^2 \cos^2 \theta \varepsilon_x^2 \right] \right. \\ \left. \cdot \left[(W_i + m_e - \omega' \sin^2 \theta')^2 \varepsilon_0'^2 + (W_i + m_e)^2 \cos^2 \theta' \varepsilon_x'^2 \right] \right\}, \quad (A-30)$$

where everything is as defined for equation (15) in the text, and the primes indicate the emitted photon. The τ_i 's are shown in Figure 1. We note the symmetry between final and initial photons. The emitted photon has the energy

$$\omega' = \frac{m_e}{\sin^2 \theta} \left(\sqrt{1 + \frac{2B}{B_0}} - \sqrt{1 + \frac{2B}{B_0} \mu'^2} \right). \quad (A-31)$$

Next we consider the scattering of an electron by an ion in an external field, first order approximation, the relativistic extension of the Born approximation. The matrix element involved in the ion's rest frame is given by equation (20); we Fourier expand the ion potential $Ze/r \cdot e^{-r/r_{sc}}$, where r_{sc} is the screening length:

$$A_0(\vec{k}) = \int \frac{d^3 k}{(2\pi)^3} e^{i\vec{k} \cdot \vec{x}} A_0(\vec{k}), \quad A_0(\vec{k}) = \frac{4\pi Ze}{k^2 + r_{sc}^{-2}} \quad (A-32)$$

Then equation (20) becomes

$$S_{fi} = \frac{-4\pi i Ze^2}{(2\pi)^3} \int \frac{d^3 k}{k^2 + r_{sc}^{-2}} \int d^4 x \overline{\psi_f(x)} \gamma^0 e^{i\vec{k} \cdot \vec{x}} \psi_i(x) \quad (A-33)$$

Substituting for ψ from equation (6) and using hermiticity gives

$$S_{fi} = -\frac{i Ze^2}{(2\pi)^3 L} [W_i(W_i + m_e) W_f(W_f + m_e)]^{-\frac{1}{2}} \int \frac{d^3 k}{k^2 + r_{sc}^{-2}} \int d^4 x f_{n_f, q_f}^*(\vec{x}_2) e^{i(W_f t - \vec{k}_2 \cdot \vec{x}_2)} U_{S_f}^+ \\ \gamma^0 (\gamma^0 \pi_\mu + m_e) \gamma^0 e^{i\vec{k} \cdot \vec{x}} (\gamma^0 \pi_\nu + m_e) U_{S_i}^- f_{n_i, q_i}(\vec{x}_2) e^{-i(W_i t - \vec{k}_2 \cdot \vec{x}_2)} \quad (A-34)$$

After moving $e^{ik \cdot x}$ to the left, we reduce the inner 4×4 to the 2×2 representation as in A-16 through A-18:

$$U_{sf}^+ \gamma^0 [\gamma^0 \pi_0 - \vec{\gamma} \cdot (\vec{\pi} + \vec{k}) + m_e] \gamma^0 (\gamma^0 \pi_0 + m_e) U_{si} \quad (A35)$$

$$= \langle s_f | [(\pi_0 + m_e)^2 + \vec{\pi} \cdot (\vec{\pi} + \vec{k}) - i \vec{\sigma} \cdot (\vec{\pi} + \vec{k}) \times \vec{\pi}] | s_i \rangle .$$

We note that $\vec{\pi} \times \vec{\pi} = \frac{1}{i} \vec{\tau} \times (e\vec{A}) = \frac{e}{i} \vec{B}$. Then substituting this expression into A-34 and assuming the initial state is the ground state gives:

$$S_{fi} = -\frac{ize^2}{(2\pi)^2 L} [w_i(w_i + m_e) w_f(w_f + m_e)]^{-\frac{1}{2}} \int \frac{d^3 k}{k^2 + r_{sc}^{-2}} \int d^4 x f_{n_f, g_f}^* e^{i(w_f t - p_f z)} e^{i\vec{k} \cdot \vec{x}} \{ \delta_{s_f, -\frac{1}{2}} [2w_i(w_i + m_e) + k^3 p_i] - \delta_{s_f, \frac{1}{2}} \sqrt{2} k^- p_i \} f_{n_i, g_i} e^{-i(w_i t - p_i z)} \quad (A36)$$

The elasticity of the interaction is expressed by the fact that the Coulomb potential had no time varying component. This results in a factor $\delta(w_f - w_i)$ in the above time integration. In evaluating the integral, we put $w_i = w_f = w$ to obtain:

$$S_{fi} = \frac{ize^2}{L} \frac{\delta(w_f - w_i)}{w(w + m_e)} \int \frac{d^3 k}{k^2 + r_{sc}^{-2}} \delta(k^3 + p_i^- - p_f^-) I_{n_f, g_f; 0, g_i}(\vec{k}_\perp) \{ \delta_{s_f, -\frac{1}{2}} [2w(w + m_e) + p_i^- (p_f^- - p_i^-)] - \delta_{s_f, \frac{1}{2}} \sqrt{2eB} e^{-i\varphi} p_i^- \} \quad (A37)$$

Substituting for the I function and carrying out the k_\perp and φ integrations gives (ignoring r_{sc}^{-2}):

$$S_{fi} = \frac{\pi i z e^2}{L} \frac{\delta(w_f - w_i)}{w(w + m_e)} \int_1^\infty \frac{d\zeta}{\zeta + \frac{(p_f^- - p_i^-)^2}{2eB}} (\zeta \sqrt{3})^{|\beta_f - \beta_i|} e^{-\zeta} \left[\frac{\min(\beta_i, \beta_f)!}{\prod_{j \neq i} \max(\beta_i, \beta_j)!} \right]^2 \delta_{s_f, g_f; +j_f} L_{\beta_f}^{(j_f)}(\zeta) \{ \delta_{s_f, -\frac{1}{2}} [2w(w + m_e) + p_i^- (p_f^- - p_i^-)] - \delta_{s_f, \frac{1}{2}} p_i^- \sqrt{2eB} j_f \} . \quad (A38)$$

We rewrite the above, noting $q_f = q_i + j_f$ and putting $j = j_f$:

$$S_{fi} = \frac{\pi z e^2}{L} i^{j+1} \frac{\delta(w_f - w_i)}{w(w+m_e)} \delta_{q_f, q_i + j} \left(\frac{q_i!}{j! q_f!} \right)^{\frac{1}{2}} \left\{ \delta_{s_f, -\frac{1}{2}} [2w(w+m_e) + p_i(p_f - p_i)] - \delta_{s_f, \frac{1}{2}} p_i \sqrt{2eBj} \right\} \int_0^\infty \frac{d\zeta}{\zeta + x} \zeta^j e^{-\zeta} L_{q_i}^{(j)}(\zeta), \quad (A39)$$

where $x = (p_f - p_i)^2 / (2eB)$. Next we square this expression, sum over final q and average over initial q according to $1/Q \sum_{q_i=0}^Q$ where Q is obtained by noting that the distance from the guiding center to the field line q is given by

$$R^2 f_{nj}(\vec{x}_\perp) = (X^+ X^- + X^- X^+) f_{nj} = \frac{eB}{2} (q + \frac{1}{2}) f_{nj}, \quad (A40)$$

The maximum q , Q , in a given area $A (= \pi R_{\max}^2)$ is given by

$$Q \approx Q + \frac{1}{2} = \frac{eB}{2} R_{\max}^2 = \frac{eBA}{2\pi}. \quad (A41)$$

The rate is obtained from

$$R_j(p_i) = \frac{1}{V} \sigma_j(p_i) |v| = \frac{1}{TQ} \sum_{q_i=0}^Q \sum_{q_f=0}^\infty \int \frac{L}{2\pi} dp_f |S_{fi}|^2. \quad (A42)$$

In the square, the δ function is handled as in A-23. The δ -function remains, and is used in the p_f integral, after

$$\delta(w_f - w_i) = \frac{w_f}{|p_f|} \sum_{\pm} \delta(p_f \pm \sqrt{p_i^2 - 2eBj}). \quad (A43)$$

Solving (A-42) for σ_j (noting that $v = p/V$) gives:

$$\sigma_j(p_i) = \frac{\pi z^2 e^4}{2eBj! |p_i p_f|} \frac{1}{(w+m_e)^2} \sum_{\pm} \left\{ \delta_{s_f, -\frac{1}{2}} [2w(w+m_e) + p_i(p_f - p_i)]^2 + \delta_{s_f, \frac{1}{2}} 2eBj p_i^2 \right\} \sum_{q_i=0}^\infty \frac{q_i!}{(q_i + j)!} \left[\int_0^\infty \frac{d\zeta}{\zeta + x} \zeta^j e^{-\zeta} L_{q_i}^{(j)}(\zeta) \right]^2. \quad (A44)$$

The sum can be re-written by using first of all the Laguerre expansion theorem (Danese, 1965, p. 517):

$$G(s) = \sum_{s=0}^{\infty} G_s^{(\alpha)} L_s^{(\alpha)}(s) \quad (A45)$$

$$G_s^{(\alpha)} = \frac{s!}{\Gamma(s+\alpha+1)} \int_0^{\infty} ds s^{\alpha} e^{-s} G(s) L_s^{(\alpha)}(s)$$

Allowing $G(s) = (\xi+x)^{-1}$ and $\alpha = j$ gives the expression

$$\sum_{j=0}^{\infty} \frac{\xi^j!}{(j+\alpha)!} \left[\int_0^{\infty} \frac{ds}{s+x} s^j e^{-s} L_j^{(j)}(s) \right]^2 = \int_0^{\infty} \frac{ds}{s+x} s^j e^{-s} \sum_{j=0}^{\infty} G_j^{(j)} L_j^{(j)}(s) \quad (A46)$$

But by A-45, we have

$$\int_0^{\infty} \frac{ds}{s+x} s^j e^{-s} \sum_{j=0}^{\infty} \hat{G}_j^{(j)} L_j^{(j)}(s) = \int_0^{\infty} \frac{ds}{(s+x)^2} s^j e^{-s} \quad (A47)$$

Finally, we obtain

$$\hat{G}_j^{(j)}(p_i) = \frac{\pi \xi^2 r_e^2}{(w+m_e)^2} \frac{B_3}{2B} \frac{1}{j!} \frac{1}{|p_i - p_f|} \sum_{\pm p_f} \epsilon_j(x_{\pm}) \quad (A48)$$

$$\cdot \left\{ \delta_{s_f, -\frac{1}{2}} [2w(w+m_e) + p_i(p_f - p_i)]^2 + \delta_{s_f, \frac{1}{2}} p_i^2 \cdot 2eBj \right\}$$

where $r_e = e^2/(mc^2)$ is the classical electron radius, and the ϵ_j are given by (putting $\xi+x = t$ in A-47):

$$\epsilon_j(x) = \int_x^{\infty} \frac{dt}{t^2} e^{-(t-x)} (t-x)^j, \quad x = \frac{(p_f - p_i)^2}{2eB} \quad (A49)$$